



AGE AND METAMORPHIC CONDITIONS OF THE GRANULITES FROM CAPRAL-JEGESSKY SYNCLINORIA, ANABAR SHIELD

Lyudmila Yu. SERGEEVA¹, Aleksei V. BEREZIN², Nikolai I. GUSEV¹, Sergei G. SKUBLOV², Aleksei E. MELNIK²

¹A.P. Karpinsky Russian Geological Research Institute, Saint-Petersburg, Russia

²Institute of Precambrian Geology and Geochronology RAS, Saint-Petersburg, Russia

The paper presents the results of the isotope, geochemical and thermobarometric study of plagio-crystalline schist containing in the Upper Anabar series of the Anabar Shield. Granulite complexes of the paleoplatforms are the most important issue in addressing the fundamental problem of the Earth's crust origin and its composition. The early stages of crust formation which correspond to the deeply metamorphosed rocks of the platform basements, available for study within the shields, are of particular interest. The study of the age and metamorphic conditions of granulites by the case of the Upper Anabar series allows specifying the stages the Anabar Shield's ancient crust formation.

Isotope-geochemical (U-Pb geochronology for zircon and Sm-Nd for garnet-amphibole-WR) and thermobarometric (Theriak-Domino) studies of plagio-crystalline schist allowed to identify two Paleoproterozoic metamorphism stages within the territory of the Anabar Shield with an age of about 1997 and 1919 million years. The peak conditions of granulite metamorphism are determined as 775 ± 35 °C and 7.5 ± 0.7 kbar, the parameters of the regressive stage are 700 °C and 7 kbar. The sequence of the rocks metamorphic transformations can be assumed: high-thermal metamorphism of the granulite facies ($T \leq 810$ °C) and subsequent sub-isobaric (about 7 kbar) cooling to 700 °C with a water activity increase and formation of Grt-Amp paragenesis corresponding to the transition from the granulite to amphibolite facies. Data on the REE and other trace elements distribution in zircon and rock-forming minerals obtained by the ion microprobe analysis contribute significantly to the isotope-geochemical data interpretation.

Key words: granulites, geochemistry, U-Pb age, Anabar Shield

How to cite this article: Sergeeva L.Yu., Berezin A.V., Gusev N.I., Skublov S.G., Melnik A.E. Age and Metamorphic Conditions of the Granulites from Capral-Jegessky Synclinoria, Anabar Shield. *Zapiski Gornogo instituta*. 2018. Vol. 229, p. 13-21. DOI: 10.25515/PMI.2018.1.13

Introduction. Granulite complexes of the paleoplatforms are the most important issue in addressing the fundamental problem of the Earth's crust origin and composition. The early stages of crust formation which correspond to the deeply metamorphosed rocks of the platform basements available for study within the shields are of particular interest. The Anabar Shield is characterized by the wide distribution of the granulite facies metamorphic rocks. The study of the age and metamorphic conditions of granulites by the case of the Upper Anabar series allows specifying the stages the Anabar Shield's ancient crust formation.

The paper presents the results of the isotope, geochemical and thermobarometric study of plagio-crystalline schist from the Upper Anabar series of the Anabar Shield.

Geological framework. The largest outcrops of the Archean granulite formations are located in the central part of the Anabar Shield (Siberian platform) where they occur in the Daldyn and Dzhelindi blocks of sub-meridional extension. The more studied Daldyn block shows, in general, the anticlinorium structure [2]. In its axial part based on the Dalynian series granulites outcrops, the Bekelekh anticlinorium was determined. The Bekelekh anticlinorium passes to the Kotoikansky synclinorium in the west and to the Kapral-Djeges synclinorium (KDS) in the east composed of granulites from the Upper Anabar series. The KDS is traced for over 200 km through the entire Anabar Shield, in the south of the Jeges River source in the north-western direction to the Kotuikan River headwater and further northward it is hidden under the platform cover. The Upper Anabar KDS series is mainly composed by hypersthene-, bipyroxene, biotite-hornblende plagiogneisses and gneisses. The interbeds of high-alumina and calc-silicate rocks are presented in combination with quartzites, magnetite-bearing crystalline schist, dioxide-scapolite and graphite-bearing gneisses. The thickest (600-800 m) and laterally extended rocks complexes are confined to the bottoms part of the Upper Anabar series. In the upper part of the section the paragneisses are less frequent and their thickness decreases. A significant part of the Upper Anabar series is presented by mafic crystalline shales forming lenticular horizons up to 600 m thick. The series is completed by the horizon of biotite-hornblende plagiogneisses with rare paragneisses interlayers. The horizon is confined to the

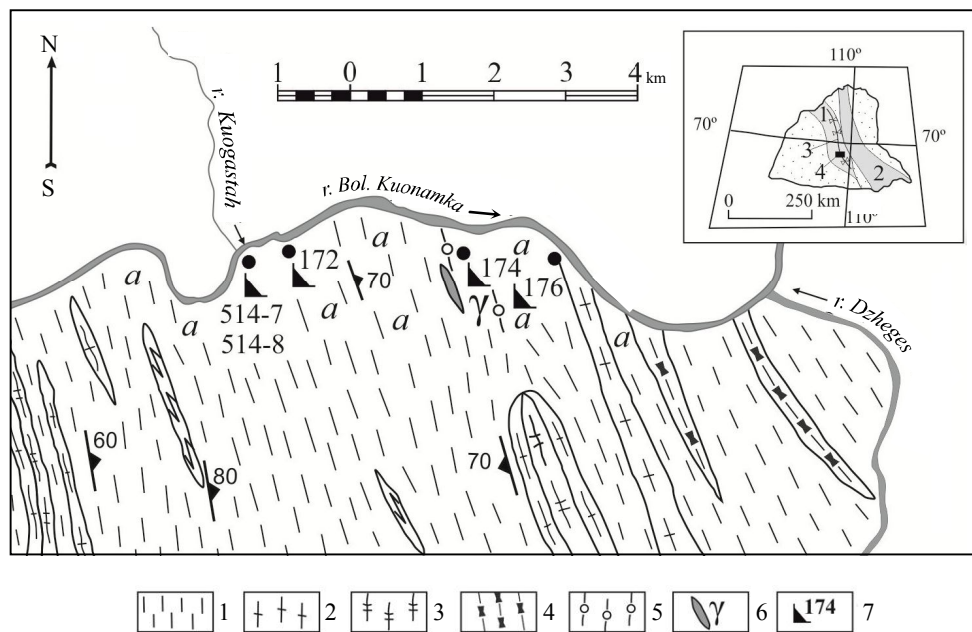


Fig.1. The geological structure of the right-hand side of the river Bol. Kuonamka in the area of its confluents Kuogastah and Dzheges (based on A.V.Berezin et. al. [2])

- 1 – bipyroxene-plagioclase melanocratic gneisses, less frequently crystalline schist; 2 – garnet, biotite-garnet, hypersthene-garnet gneisses and plagiogneisses; 3 – amphibolites and amphibole crystalline schists; 4 – quartzite and quartzite schists; 5 – garnet-bearing crystalline schists; 6 – alaskite granites; 7 – sampling points for isotope dating
- The sidebar shows the outline of the Anabar shield and the granulites range within: 1 – Daldyn block; 2 – The Dzhelendin block; 3 – axis of the Dzheges synclinorium; 4 – studied area

core of the Kapral-Dzheges synclinorium and is especially well traced in the interfluvium of the Bol. Kuonamka and Jeges rivers. This particular synclinorium core was examined on the right-hand side of the river Bol. Kuonamka from the mouth of its left confluent Kuogastah to approximately 7 km downstream to the mouth of the Dzheges river (Fig.1).

The studied area is distinguished by the extremely monotonous rock set. Dark gray and brownish quartz-bearing melanocratic bipyroxene-plagioclase crystalline schist with a schlieren texture, sometimes turning into mafic lenticular-banded crystalline schist prevail almost everywhere. In the migmatitic species, a coarse banding crushed into simple open folds, with leucosome lenticular areas in the fold hinges. Leucosome is represented by enderbites (hypersthene plagiogneisses), also involved in folding. The thickness increase is specific to enderbites located in the cores of the antiform folds. Occasionally, there are garnet-bearing crystalline schist with small garnet aggregates up to 1.5 cm across surrounded by quartz-plagioclase leucocratic intergrowth. In addition, elongated garnet grains are at times included in polysynthetically twinned plagioclase grains. There is no clinopyroxene in the garnet-bearing crystalline schist, and garnet coexists with orthopyroxene only. The imposed amphibolization appears as isolated hornblende areas (brownish in thin sections), varying in size from the first centimeters to lenticular amphibolite segregations, sometimes up to 1 m in diameter, composed of medium-grained hornblende and a plagioclase in various amounts, up to its complete absence. Hornblende replaces both pyroxenes and garnets.

The chemical composition of the main granulites corresponds to the magnesian and meta-alumina mafic rocks of the tholeiitic series, with low and moderate potassium content (K_2O – 0.36-0.87 %, mg# 35-51; A/NK = 2.45-3.20; A/CNK = 0.69-0.92).

Analytical methods. The garnet-orthopyroxene plagiocrystalline schist from the Upper Anabar series was under detailed isotope geochemical study. The composition of rock-forming minerals was determined at the Institute of Precambrian geology and geochronology RAS (by O.L.Galankina) using a JEOL JSM-6510LA scanning electron microscope with an energy dispersive detector JED-2200. The zircon U-Pb dating was carried out in the A.P.Karpinsky Russian Geological Research Institute on the SHRIMP-II ion microprobe by standard methods. The content of REE and



other trace elements in zircon and rock-forming minerals was determined on the ion microprobe analyzer Cameca IMS-4f in the Yaroslavl Branch of the Institute of Physics and Technology (by S.G.Simakin, E.V.Potapov) using the released methods [4, 5, 9]. The zircon chemical composition was analyzed at the particular points of previous U-Pb dating. In the REE spectra scheduling, the composition of zircon and rock-forming minerals was normalized to the chondrite CI composition [12]. The list of mineral abbreviations is given in Ref. [18].

Results.

Minerals composition. The garnet-orthopyroxene plagiocrystalline schist (sample 174) is composed of Pl (53%), Amp (32%), Opx (10%), Grt (4%). Subhedral plagioclase grains reach 0.5 mm in diameter and correspond to andesine with anorthite content up to 43%. All K-feldspar grains contain about 5% albite components and adjoin smaller (up to 0.2 mm) plagioclase grains.

The composition of orthopyroxene euhedral grains which are up to 0.5 mm in size is a mixture of ferrosilicon and enstatite in equal proportions with an insignificant value of the wollastonite component. The Al content in orthopyroxene does not exceed 0.1 apfu. Clinopyroxene with a magnesia component exceeding 0.6 is almost always associated with orthopyroxene and contains no more than 6% of the jadeite component.

The xenomorphic garnet aggregates probably fill out a weakened zone (cracks) with a thickness of up to 1 mm. There is also single garnet grains formed inside the plagioclase matrix together with amphibole. The pyrope-grossular-almandine composition of garnet is specified by Alm component of about 60% with an increased content of Sps component – 4%, which indicates retrograde metamorphic conditions. The Grs component (17-19%) prevails over Py (14-17%).

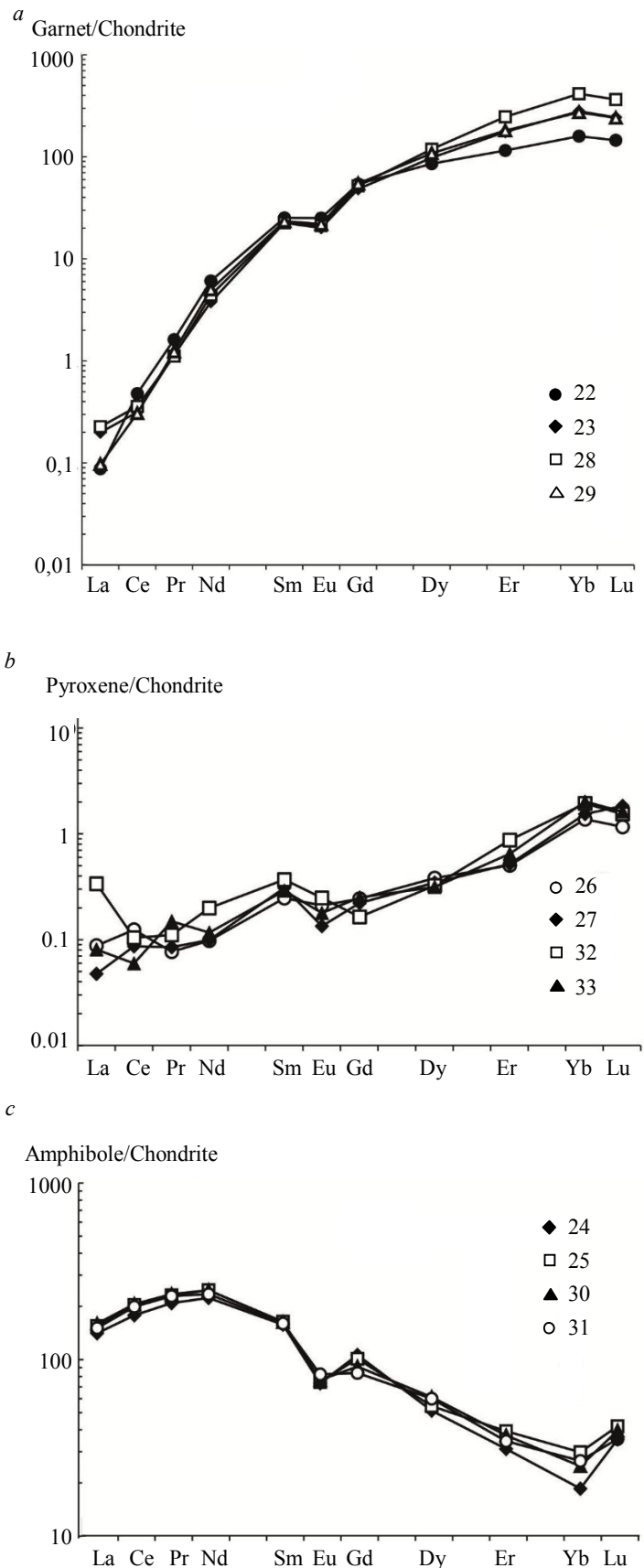


Fig.2. REE distribution spectra in garnets (a), pyroxenes (b) and amphiboles (c) from garnet-orthopyroxene plagiocrystalline schist (sample 174)
The points numbers correspond to Table 1

The garnet crystals are generally homogeneous in the CaO, FeO, MnO, and MgO distribution. There is only a slight decrease in the MnO content from core to rim. Zoning of this type tends to be characteristic for garnets formed at high metamorphic grade settings [1] and also implies retrograde formation.

Amphibole replacing pyroxenes with magnesia content of about 0.5 refers to the calcium group and can be represented as a mixture of 70 % pargasite, 20 % ferrotschermakite and 10% glaucophane components. Amphiboles of this composition are characteristic of the amphibolite facies metamorphism, which does not contradict its paragenesis with a garnet, rich in an almandine component.

REE in minerals. The rare earth elements study of garnets from plagiocrystalline schist revealed typical enrichment in HREE with a minimum at Eu ($Eu/Eu^* = 0.63$) (Fig.2, a). There is no zoning for LREE and HREE within the garnet crystals, but only enrichment in HREE in going from core to rim.

The distribution of REE in orthopyroxenes is slightly differentiated (Fig.2, b) with the total REE content not exceeding 1 ppm. The magnitude of the Eu anomaly varies up to its disappearance ($Eu/Eu^* = 0.51-1.01$).

The total content of REE in amphibole is 334-371 ppm with the predominance of LREE (291-327 ppm), significant differentiation ($(La/Yb)_N = 5.19-7.59$), and moderate negative Eu-anomaly ($Eu/Eu^* = 0.57-0.71$) (Fig.2, c). Amphibole is also characterized by increased contents of Ti (17997-20704 ppm), V (495-700 ppm), and Zr (127-172 ppm) (Table 1).

Table 1

The content of major (wt%), trace and rare-earth elements (ppm) in garnets, orthopyroxenes and amphiboles from plagiocrystalline schist (sample 174)

Compound/ element	Garnet				Orthopyroxene				Amphibole			
	22 core	23 rim	28 rim	29 rim	26	27	32	33	24	25	30	31
SiO ₂	37.6	38.0	37.7	38.3	51.0	50.8	50.0	50.7	42.1	41.8	42.6	42.0
TiO ₂	–	–	–	–	–	–	–	–	2.59	2.40	2.99	2.81
Al ₂ O ₃	21.9	21.5	21.4	20.8	0.76	1.32	1.28	1.14	13.0	13.2	12.4	12.4
FeO	27.7	27.9	28.5	28.1	30.1	29.9	31.0	30.8	17.9	18.2	17.8	18.9
MnO	1.65	2.03	2.18	1.87	0.71	0.73	0.71	0.69	0.32	0.18	–	0.27
MgO	4.15	3.81	3.99	4.25	16.9	16.8	16.6	16.0	9.29	9.14	9.23	9.29
CaO	6.92	6.80	6.25	6.65	0.47	0.48	0.46	0.60	11.5	11.9	11.6	11.1
Na ₂ O	–	–	–	–	–	–	–	–	1.79	1.67	1.88	1.63
K ₂ O	–	–	–	–	–	–	–	–	1.59	1.55	1.58	1.49
La	0.02	0.05	0.05	0.02	0.02	0.01	0.08	0.02	33.4	36.7	37.9	35.7
Ce	0.29	0.19	0.22	0.19	0.08	0.05	0.06	0.04	109	125	126	122
Pr	0.15	0.11	0.10	0.11	0.01	0.01	0.01	0.01	19.3	21.4	21.8	21.2
Nd	2.78	1.73	2.02	2.29	0.04	0.05	0.09	0.05	102	113	113	107
Sm	3.73	3.33	3.36	3.47	0.04	0.05	0.05	0.04	23.3	24.2	24.1	23.7
Eu	1.42	1.13	1.19	1.24	0.01	0.01	0.01	0.01	4.13	4.20	4.32	4.64
Gd	10.8	9.62	10.3	10.9	0.05	0.04	0.03	0.05	21.1	20.1	18.2	16.7
Dy	21.1	24.1	29.3	26.6	0.09	0.09	0.08	0.08	12.6	13.4	15.1	14.8
Er	18.5	28.1	39.6	28.9	0.08	0.08	0.14	0.10	4.99	6.28	5.94	5.51
Yb	25.6	45.0	66.8	43.9	0.22	0.25	0.31	0.33	2.99	4.80	4.01	4.29
Lu	3.57	6.00	8.99	5.91	0.03	0.05	0.04	0.04	0.87	1.03	0.97	0.87
Ti	508	248	292	354	487	619	515	596	17997	18248	20704	20302
V	120	121	113	123	57.9	83.3	68.9	77.3	658	700	518	495
Cr	49.5	44.5	68.4	75.9	151	156	146	150	147	161	152	133
Sr	0.38	0.54	0.31	0.28	0.50	0.26	0.57	0.25	141	185	189	211
Y	177	227	288	238	0.59	0.60	0.79	0.82	50.9	61.8	61.4	61.0
Zr	21.8	13.0	15.4	16.6	2.44	4.13	2.53	2.88	127	172	156	171



End of Table 1

Compound/ element	Garnet				Orthopyroxene				Amphibole			
	22 core	23 rim	28 rim	29 rim	26	27	32	33	24	25	30	31
Nb	0.05	0.04	0.04	0.02	0.03	0.04	0.04	0.04	23.3	25.7	28.9	28.1
Hf	7.05	8.20	9.19	8.00	0.08	0.08	0.12	0.10	7.58	8.98	8.51	8.28
Eu/Eu*	0.68	0.61	0.62	0.61	0.86	0.51	1.01	0.66	0.57	0.58	0.63	0.71
(La/Yb) _N	0.0006	0.0007	0.0005	0.0004	0.06	0.03	0.17	0.04	7.59	5.19	6.42	5.65
(Sm/Nd) _N	4.14	5.96	5.12	4.67	2.53	3.11	1.85	2.50	0.71	0.66	0.66	0.68
(Yb/La) _N	1814	1405	1831	2805	15.6	32.4	5.75	25.1	0.13	0.19	0.16	0.18
∑REE	88.0	119	162	124	0.67	0.68	0.92	0.77	334	370	371	357
∑HREE	79.6	113	155	116	0.47	0.51	0.60	0.60	42.6	45.6	44.1	42.1
∑LREE	8.40	6.54	6.95	7.33	0.20	0.17	0.31	0.18	291	324	327	314

Dash - the element content is b.d.l.

Sm-Nd isotopic data. Sm-Nd isotopic data for whole rock and bulk garnet, clinopyroxene, and amphibole probes were analyzed using TIMS method, with an error $\pm 0.5\%$ on a multicolumn mass spectrometer TRITON in the IPGG RAS. The mineral grains were separated using heavy liquids, with subsequent handpicking under a binocular microscope (about 100 mg of garnet, clinopyroxene, and amphibole).

The inclusions with low Sm/Nd ratio (apatite, monazite, and others) frequently occur in garnet, affect the accuracy of the Sm-Nd dating [15]. Therefore, selective digestion of possible inclusions with low Sm/Nd ratio included the sulphuric acid leaching technique. This technique used here for the garnets, preliminary crushed in an agate mortar, consists of only one step: leaching for 24-25 hours at 180 °C in 96 % H₂SO₄ [6]. This processing method significantly increases the range of ¹⁴⁷Sm/¹⁴⁴Nd ratio variations, hence, the accuracy of dating [3]. The isochron construction, as well as the age calculation, was carried out in the Isoplot toolkit [11].

A garnet-orthopyroxene plagiocrystalline schist (sample 174) yields a three-point isochron (WR, Amp, Grt) corresponding to an age of 1919 \pm 13 Ma (MSWD = 0.75, Fig.3).

The addition of orthopyroxene isotopic data to the age calculations do not affect the Sm-Nd age (1914 \pm 49 Ma) but increases the MSWD value to 13.

Zircon geochemistry and U-Pb age.

Zircon from garnet-orthopyroxene plagiocrystalline schist (sample 174) is represented by grains with smoothed ribs with an elongation ratio 1.3-2.7. Grains are gray and dark gray in CL with prevalent sector zoning and also shaded thin-banded growth zoning (Fig.4).

A concordant age of 1997 \pm 10 Ma was obtained by U-Pb zircon dating (10 measurements) (Fig.4). Zircon of the Paleoproterozoic age is characterized by a low and average U (106-394 ppm) and low Th (mean value is 66 ppm) contents. The Th/U ratio mean value is 0.31 (Table 2).

The mean value of REE content in zircon is 520 ppm and shows HREE enrichment with positive Ce-anomaly and negli-

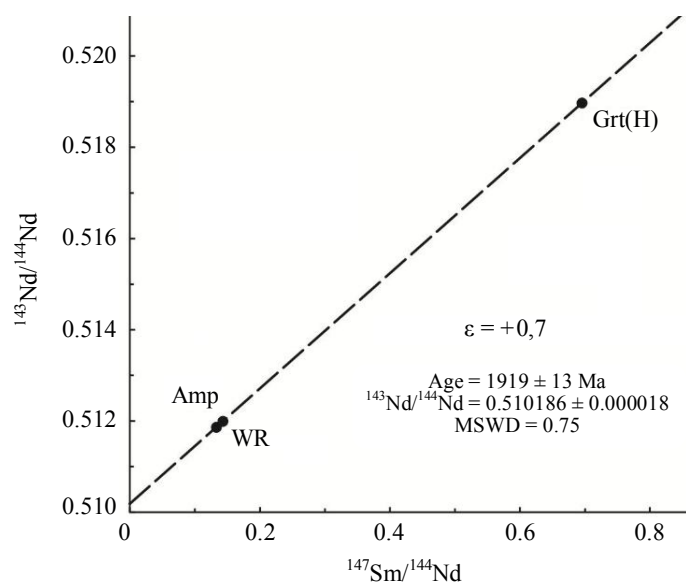


Fig.3. Sm-Nd isochron for garnet-orthopyroxene plagiocrystalline schist (sample 174)
WR – whole rock; Amp – amphibole;
Grt (H) – garnet after the sulfuric acid leaching

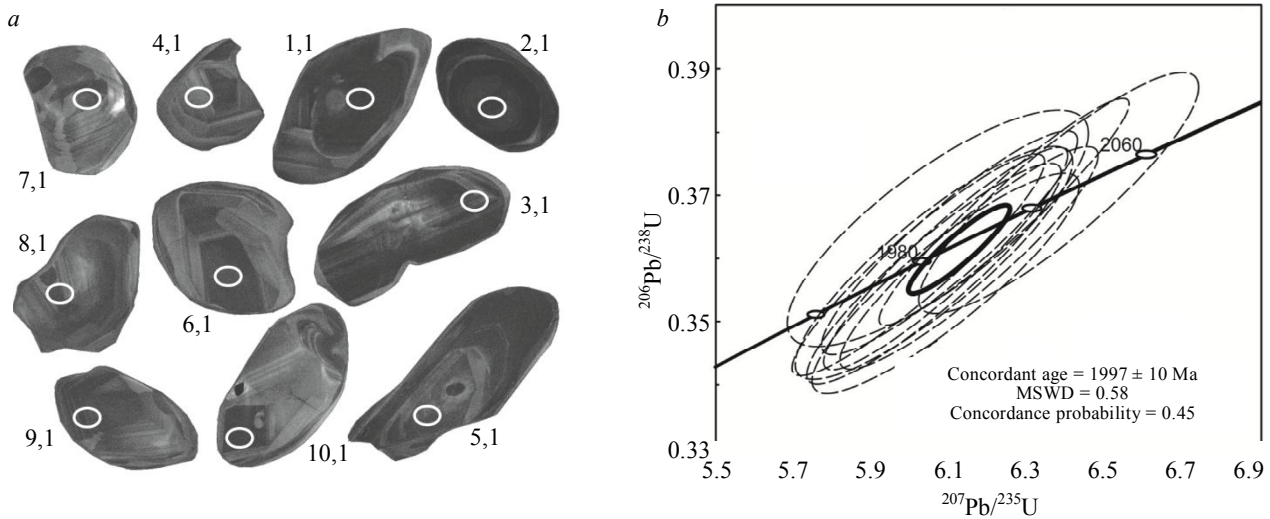


Fig.4. CL images (a) and concordia diagram (b) of zircon from garnet-orthopyroxene plagiocrystalline schist.
Ellipses dimensions are in the 2 σ interval

gible negative Eu-anomaly (mean value $Eu/Eu^* = 0.43$) (Fig.5, a). The LuN/LaN ratio varies over a wide range of values from 871 to 9672 (except analytical points 5,1 and 8,1). Zircon Hf content mean value is 7351 ppm, while Y, P and Ca concentrations are variable (Table 2).

Zircon yields almost constant Ti contents of the mean value 11 ppm. The average value of calculated Ti-in-zircon temperature is 755 °C [16], which corresponds to the parameters of the granulite facies metamorphism.

Table 2

The content of trace and rare-earth elements (ppm) in zircon from garnet-orthopyroxene from plagiocrystalline schist (sample 174)

Compound/ element	Analytical point number (Fig.4, a)									
	1,1	2,1	3,1	4,1	5,1	7,1	8,1	9,1	10,1	
La	0.03	0.08	0.80	0.15	1.01	0.08	0.04	0.13	1.11	
Ce	2.33	10.5	9.45	4.26	8.10	6.78	5.16	7.52	13.8	
Pr	0.01	0.21	0.51	0.10	0.75	0.35	0.06	0.39	0.32	
Nd	0.07	2.71	4.18	0.79	4.21	4.44	0.70	5.02	2.55	
Sm	0.15	2.88	3.90	1.27	1.29	5.88	1.13	5.95	3.06	
Eu	0.04	0.91	1.11	0.34	0.58	1.53	0.38	1.51	0.86	
Gd	1.28	13.7	17.4	6.05	4.19	23.8	5.32	26.1	14.7	
Dy	6.37	54.2	68.4	24.5	15.3	79.2	23.6	90.8	78.0	
Er	23.2	147	178	64.8	46.3	179	79.2	206	264	
Yb	77.9	398	406	167	129	372	250	430	614	
Lu	17.1	76.6	72.7	31.8	26.8	67.6	54.0	77.8	116	
Li	5.23	2.40	2.63	0.79	4.45	0.39	3.46	0.70	3.58	
P	22.6	105	191	61.2	75.7	166	72.3	89.0	512	
Ca	0.16	0.39	13.1	0.94	24.0	0.52	1.27	1.03	311	
Ti	13.3	11.7	8.44	14.0	7.65	9.69	11.6	14.5	10.3	
Sr	0.08	0.27	0.67	0.19	0.82	0.41	0.33	0.33	1.81	
Y	121	954	1026	371	260	1056	433	1161	1383	
Nb	145	122	84.7	73.7	95.2	66.3	47.6	46.1	41.1	
Ba	1.35	0.97	1.69	1.02	2.30	1.55	0.54	0.82	0.60	
Hf	7450	8697	6873	6820	8925	6362	7142	7119	6768	
Th	19.2	194	118	29.6	42.3	97.2	64.7	120	163	
U	376	743	426	136	328	266	378	329	668	
Th/U	0.05	0.26	0.28	0.22	0.13	0.37	0.17	0.37	0.24	
Eu/Eu*	0.30	0.44	0.41	0.38	0.76	0.39	0.47	0.37	0.39	
Ce/Ce*	28.1	19.8	3.57	8.20	2.26	10.0	25.7	8.17	5.60	

Compound/ element	Analytical point number (Fig.4, a)								
	1,1	2,1	3,1	4,1	5,1	7,1	8,1	9,1	10,1
ΣREE	129	707	762	301	237	740	419	852	1109
ΣLREE	2.44	13.5	14.9	5.30	14.1	11.7	5.96	13.1	17.8
ΣHREE	126	690	742	294	221	721	412	831	1087
Lu _N /La _N	5301	9672	871	2002	256	8429	12576	5905	1003
Lu _N /Gd _N	109	45.3	33.7	42.5	51.8	22.9	82.1	24.1	63.7
Sm _N /La _N	7.84	60.5	7.77	13.3	2.04	122	43.8	75.0	4.41
T(Ti), °C	769	757	728	774	720	740	756	777	746

The zircon points on the La-(Sm/La)_N diagram [10, 14] fall into the fields of unaltered magmatic and porous zircons (Fig.5, b). The distinctive features of porous zircon are the increased content of La, Fe, Ca, Al and an abnormally low (Sm/La)_N ratio [9]. At points 3.1 and 5.1. Ca content is noticeably higher than in unaltered zircons (Table 2), and at point 10.1 this value reaches 311 ppm with also low (Sm/La)_N ratio = 2-8.

PT-parameters of metamorphism. Sample 174 is chosen for the metamorphism parameters study since it contains garnet phase, which substantially increases the number of the reactions suitable for the temperature calculation. The TWQ method gives T= 695±15 °C and P = 6±1 kbar (based on three independent reactions) for the late paragenesis of Amp-Grt-Pl-Qz. Obtained PT parameters correspond to the boundary conditions of the amphibolite and granulite facies [13] and, as can be seen, are characterized by the incomplete equilibrium of coexisting minerals (Fig. 6).

The equilibrium is incomplete because amphibole defining pressure-dependent reaction (e.g. 3Ab + 2Gr_s + Prp + 3Ts = 3Prg + 6bQtz + 6An and 3Ab + 2Gr_s + Prp + 4Ts = 3fPrg + T + 6bQtz + 6An) and garnet, determining a temperature (e.g. 3Prg + 4Alm = 4Prp + 3fPrg) formed with a certain time interval. An additional point is that significant uncertainty makes the inaccuracy of the thermodynamic parameters for the amphibole group end members. The water activity in the system was not less than 0.8, which is consistent with the observed orthopyroxene and amphibole phase's ratios.

To verify the obtained P-T values. pseudo-section and isopleths calculations were performed using Theriak-Domino software package with the JUN92d.bs database, which is an analog of the thermodynamic database used in TWQ [17]. Since a local inhomogeneity in the minerals distribution and composition is not rare in polymetamorphic rock complexes, the most appropriate method

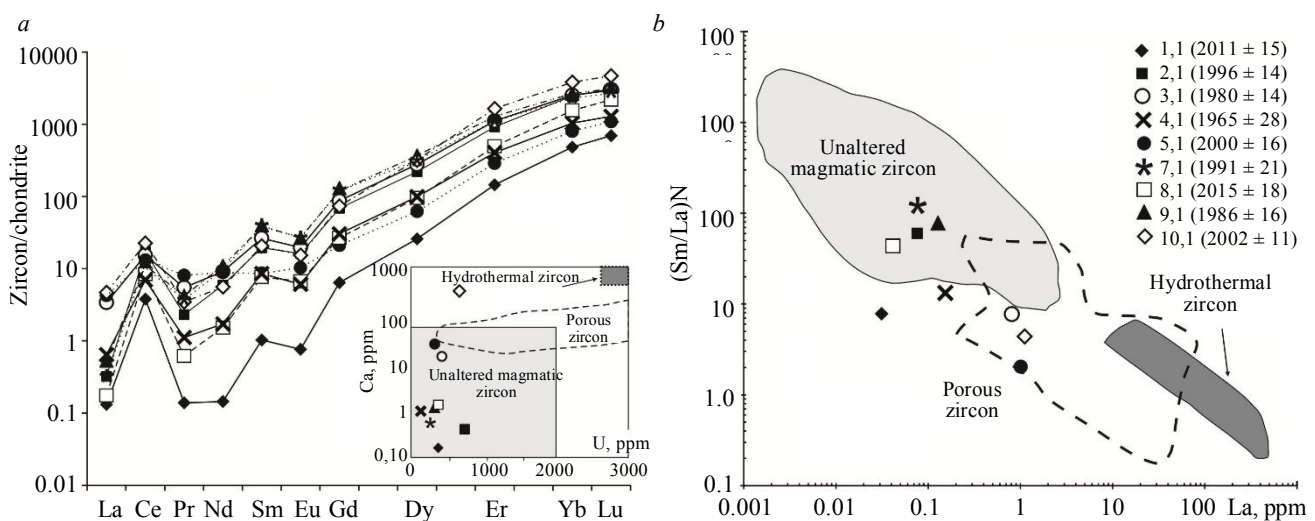


Fig.5. The distribution of REE (a) in zircon from a garnet-orthopyroxene plagiocrystalline schist (sample 174) and the position of zircon figurative points on discrimination diagrams (b)

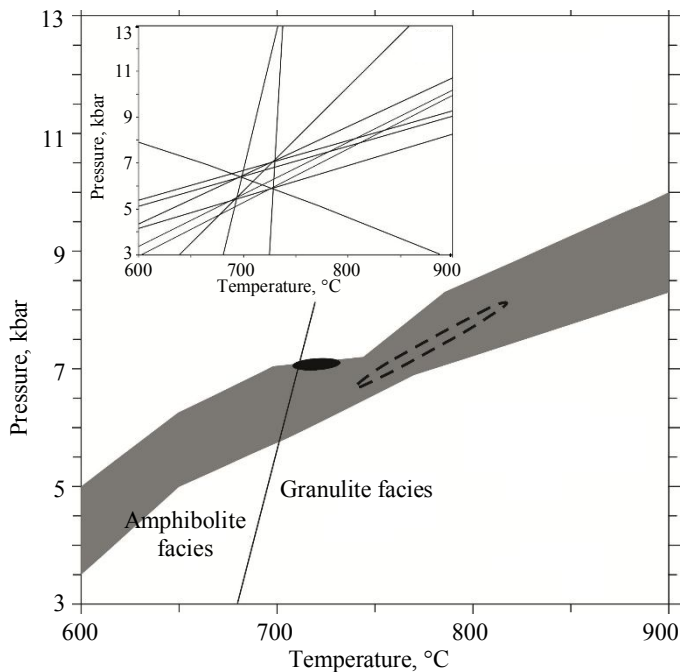


Fig.6. The stability field of mineral paragenesis in sample 174 (gray fill), calculated in the Theriak-Domino software package [8] for the MnNCMFATSH system at $a_{H_2O} = 0.8$. The regions of the minimum PT-parameters (~ 720 °C и 7 kbar) for the Grt + Opx + Pl + Amp association and the maximum PT-parameters (~ 775 °C и 7,5 kbar) for the Opx + Pl association are shown by ellipses (black fill and bold dotted line, correspondingly). The boundaries of the amphibolite and granulite facies are shown by Oh and Liou [13]. The sidebar shows the convergence of the mineral reaction lines for the Grt + Opx + Pl + Amp association, calculated in the TWQ program [7]

for estimating the rock's bulk composition with equilibrium mineral paragenesis is to calculate it by the actual minerals compositions ratios. The isopleths of garnet (Alm, Py, Grs) and plagioclase (An) end members, magnesia and Al content in orthopyroxene (apfu) were calculated and constructed by the actual method. Further, with a comparison of the calculated compositions and measured ones, was constructed a rather compact region (the black ellipse in Fig.6), showing the area, where minerals compositions are the closest. The obtained PT-parameters (720 ± 10 °C. 7.0 ± 0.2 kbar) are almost equal to the TWQ ones.

The evaluation of the early high-temperature metamorphism PT-parameters is a much more complex task since only the most basic plagioclase and orthopyroxene with maximum alumina content can be assigned to the minerals, formed in this conditions. Using the principle of effective bulk composition [8] corresponding to the retrograde metamorphism, garnet and amphibole were removed from the calculations. Then iso-

pleths for the anorthite component in plagioclase, and the tschermakite component and magnesia in orthopyroxene were calculated. Using the above-described method, a region corresponding to the maximum PT-parameters (dotted ellipse in Fig.6) with a temperature of 775 ± 35 °C and a pressure of 7.5 ± 0.7 kbar was constructed. This approximate estimate indicates that the protolith at an early stage experienced metamorphism under granulite-facies conditions. The additionally calculated area of coexistent real mineral paragenesis (gray fill in Fig.6) indicates the possibility of observed paragenesis formation in the extended in temperature, but limited in pressure interval.

Thus, the sequence of the rock metamorphic transformations can be traced: high-thermal granulite facies metamorphism ($T \leq 810$ °C and subsequent sub-isobaric (about 7 kbar) cooling to 700 °C with the water activity increase and Grt-Amph paragenesis formation, corresponding to the granulite to amphibolite facies transitional phase [13].

Conclusions. The detailed study of plagio-crystalline schist from the Upper Anabar series provides new information on the age, geochemical features, and PT-conditions of the rocks formation. The plagio-crystalline schist protolith is the basic rock not containing primary magmatic zircon. The age of 1997 ± 10 Ma, obtained by the U-Pb zircon dating corresponds to the time of granulite facies metamorphism. Sm-Nd age of 1919 ± 13 Ma obtained from the whole rock, bulk garnet, and amphibole probes indicates the regressive amphibolite facies metamorphism. The granulite facies metamorphism peak conditions are determined as 775 ± 35 °C and 7.5 ± 0.7 kbar. The regressive stage of metamorphism, which led to the Grt-Amph paragenesis formation, occurred at the temperature of about 700 °C and pressure of 7 kbar.

Acknowledgements. The authors are grateful to O.L.Galankina, E.S.Bogomolov (IPGG RAS), S.G.Simakin, E.V.Potapov (IPT RAS) and colleagues of the VSEGEI Institute for analytical studies. The study was carried out with the financial support of the Russian Foundation for Basic Research (grants 17-35-50002, 16-35-60092, 18-35-00229).



REFERENCES

1. Avchenko O.V. Petrogenetic informative features of garnets from metamorphic rocks. M.: Nauka, 1982. 100 p (in Russian).
2. Geological Map of the USSR on a Scale 1:200000. Anabar Series. Sheets R-49-XIX, XX. Explanatory Notes. Ed. by A.A.Poturoev. Moscow, 1984. 82 p (in Russian).
3. Berezin A.V., Travin V.V., Marin Y.B., Skublov S.G., Bogomolov E.S. New U-Pb and Sm-Nd ages and PT estimates for eclogitization in the Fe-rich gabbro dyke in Gridino area (Belomorian Mobile Belt). *Doklady Earth Sciences*. 2012. Vol. 444. N 2, p. 760-765 (in Russian).
4. Sobolev A.V., Batanova V.G. Mantle lherzolites of the Troodos ophiolite complex, Cyprus – clinopyroxene geochemistry. *Petrology*. 1995. Vol. 3, N 5, p. 440-448 (in Russian).
5. Fedotova A.A., Bibikova E.V., Simakin S.G. Ion-microprobe zircon geochemistry as an indicator of mineral genesis during geochronological studies. *Geochemistry International*. 2008. Vol. 46. N 9, p. 912-927 (in Russian).
6. Anczkiewicz R., Thirlwall M.F. Improving precision of Sm-Nd garnet dating by H₂SO₄ leaching: a simple solution to the phosphate inclusion problem. *Geochronology: Linking the isotopic record with petrology and textures. Journal of Geological Society London. Special Publications*. 2003. Vol. 220, p. 83-91.
7. Berman R.G. Thermobarometry using multi-equilibrium calculations: a new technique, with petrological applications. *Canadian Mineralogist*. 1991. Vol. 29, p. 833-855.
8. De Capitani C., Petrakakis K. The computation of equilibrium assemblage diagrams with Theriak/Domino software. *American Mineralogist*. 2010. Vol. 95, p. 1006-1016.
9. Hinton R.W., Upton B.G.J. The chemistry of zircon: Variations within and between large crystals from syenite and alkali basalt xenoliths. *Geochimica et Cosmochimica Acta*. 1991. Vol. 55, p. 3287-3302.
10. Hoskin P.W.O. Trace-element composition of hydrothermal zircon and the alteration of Hadean zircon from the Jack Hills, Australia. *Geochimica et Cosmochimica Acta*. 2005. Vol. 69, p. 637-648.
11. Ludwig K.R. ISOPLOT/Ex – A geochronological toolkit for Microsoft Excel, Version 2.05. Berkeley Geochronology Center Special Publication. 1999. N 1a. 47 p.
12. McDonough W.F., Sun S.S. The composition of the Earth. *Chemical Geology*. 1995. Vol. 120, p. 223-253.
13. Oh C.W., Liou J.G. A petrogenetic grid for eclogite and related facies under high-pressure metamorphism. *Island Arc*. 1998. Vol. 7, p.36-51.
14. Grimes C.B., John B.E., Cheadle M.J., Mazdab F.K., Wooden J.L., Swapp S., Schwartz J.J. On the occurrence, trace element geochemistry, and crystallization history of zircon from in situ ocean lithosphere. *Contributions to Mineralogy and Petrology*. 2009. Vol. 158, p. 757-783.
15. Scherer E.E., Cameron K.L., Blichert-Toft J. Lu-Hf garnet geochronology: closure temperature relative to the Sm-Nd system and the effects of trace mineral inclusions. *Geochimica et Cosmochimica Acta*. 2000. Vol. 64, p. 3413-3432.
16. Watson E.B., Wark D.A., Thomas J. Crystallization thermometers for zircon and rutile. *Contributions to Mineralogy and Petrology*. 2006. Vol. 151, p. 413-433.
17. Wei C. Calculated phase relations in high-pressure metapelites in the system NKFMAH (Na₂O-K₂O-FeO-MgO-Al₂O₃-SiO₂-H₂O). *Journal of Petrology*. 2004. Vol. 45, p. 183-202.
18. Whitney D.L., Evans B.W. Abbreviations for names of rock-forming minerals. *American Mineralogist*. 2010. Vol. 95, p. 185-187.

Authors: **Lyudmila Yu. Sergeeva**, Leading Engineer, Ludmila_Sergeeva@vsegei.ru (A.P. Karpinsky Russian Geological Research Institute, Saint-Petersburg, Russia), **Aleksei V. Berezin**, Candidate of Geological and Mineralogical Sciences, Research, berezin-geo@yandex.ru (Institute of Precambrian Geology and Geochronology RAS, Saint-Petersburg, Russia), **Nikolai I. Gusev**, Head of Eastern Siberia ores Department, Nikolay_Gusev@vsegei.ru (A.P. Karpinsky Russian Geological Research Institute, Saint-Petersburg, Russia), **Sergei G. Skublov**, Doctor of Geological and Mineralogical Sciences, Professor, Chief Researcher, skublov@yandex.ru (Institute of Precambrian Geology and Geochronology RAS, Saint-Petersburg, Russia), **Aleksei E. Melnik**, Candidate of Geological and Mineralogical Sciences, Junior Researcher, aleks@melnik.me (Institute of Precambrian Geology and Geochronology RAS, Saint-Petersburg, Russia).

The article was accepted for publication on 22 January, 2018.